Surface modes of a sphere coupled to a semi-infinite medium

1991 J. Phys.: Condens. Matter 3 7857

(http://iopscience.iop.org/0953-8984/3/40/007)

J. Phys.: Condens. Matter 3 (1991) 7857–7866. Printed in the UK

Surface modes of a sphere coupled to a semi-infinite medium

John S Nkoma†
International Centre for Theoretical Physics, Trieste, Italy

Received 3 August 1990, in final form 30 April 1991

Abstract. The surface modes of a sphere coupled to a semi-infinite medium are studied. We obtain a relationship which describes the dependence of frequency on the distance between the sphere and the semi-infinite medium. Our results reduce to previously reported results in the limit of a very large separation between the sphere and the semi-infinite medium. Two surface modes for each order n are shown to exist. The theory is applied to three cases: first, a metallic sphere in vacuum coupled to a semi-infinite metal of the same material; second, a metallic sphere embedded into a semi-infinite metal bounded by vacuum; third, a spherical cavity inside a semi-infinite metal bounded by vacuum.

1. Introduction

Over the past two decades, much effort has been directed towards understanding the properties of *surface* modes in various configurations of samples. For example, several aspects of surface excitations have been reviewed by Agranovich and Mills (1982), Agranovich and Loudon (1984) and Cottam and Tilley (1989). In addition to surface excitations propagating along planar interfaces of semi-infinite media, thin films, bilayers and superlattices, there is also interest in surface excitations propagating along rough surfaces and curved surfaces, for example spherical crystals (Ruppin and Englman 1970). In this paper, we shall study the properties of surface modes of a sphere coupled to a semi-infinite medium (hereafter to be referred to as SCSIM). Earlier studies of this geometry include the work of Rendell *et al* (1978), Aravind and Metiu (1983), Ruppin (1983) and Takamori *et al* (1987). We embark on this study for several reasons—the first being the need to improve on what has been known from the earlier studies mentioned previously. In the earlier studies on this geometry, the approach was based on obtaining recursion relations which could only be solved by numerical truncation. In this paper we obtain an expression that relates the frequency of surface modes of an SCSIM system to the distance between the sphere and the interface of the semi-infinite medium, and we show that there are two surface modes for each order n. Second, the geometry of the SCSIM system is important since it models several systems of practical interest, and the basic understanding of this model is of technological interest. Some systems that can be modelled by the SCSIM geometry are

† Permanent address: Physics Department, University of Botswana, Private Bag 0022, Gaborone, Botswana.

small particles coupled to tunnel junctions (Rendell *et al* 1978), molecules adsorbed on a surface in surface enhanced Raman scattering (Fleischmann *et al* 1974, Udagawa *et al* 1981, Aravind *et al* 1983, Otto 1984, Moskovits 1985, Takamori *et al* 1987), embedded atom studies for granular Ag and Au films (Cohen *et al* 1973) and particle surface interactions which are the basis of many of the modern techniques of spectroscopy (Otto 1984). The experimental tools that can be used to study the SCSIM geometry include Raman scattering, as mentioned earlier, infrared spectroscopy (Johnson *et al* 1974), and the new non-contact stylus microscopies such as scanning tunnelling microscopy (STM) (see, for example, Binnig and Rohrer 1984) and scanning near-field optical microscopy (SNOM) (see, for example, Fischer and Pohl (1989)).

The plan of this paper is as follows. In section 2, we obtain the electric potentials in various regions of the SCSIM system by solving Laplace's equation in bispherical coordinates. Application of boundary conditions enables us to obtain a result that relates the frequency of the surface modes of an SCSIM system to the distance between the sphere and the interface of the semi-infinite medium. Section 3 is devoted to numerical results and discussion, and we apply the theory developed in section 2 to three cases of practical interest. First, we consider a metallic sphere coupled to a metal of the same material occupying a semi-infinite medium; second, a metallic sphere embedded into a semi-infinite metal bounded by vacuum; and third, a spherical cavity inside a semi-infinite metal bounded by vacuum. Concluding remarks are made in section 4.

2. The frequency–distance relation for an SCSIM system

The geometry of the SCSIM system is illustrated in figure 1. A sphere of radius R with a dielectric function ϵ_1 occupies region I which is embedded in region II with a dielectric function ϵ_2, and region III ($z < 0$) has a dielectric function ϵ_3. Depending on which of the dielectric functions is frequency-dependent (active medium) and which is frequency independent (inactive medium), there are several possible applications of the SCSIM geometry, and we shall consider three cases illustrated in figures 2(a) to (c). In figure 2(a), a metallic sphere in vacuum is coupled to a metal of the same material occupying a semi-infinite medium, while in figure 2(b) a metallic sphere embedded into a semi-infinite metal bounded by vacuum is considered and finally in figure 2(c) a spherical cavity inside a semi-infinite metal bounded by vacuum is illustrated.

The following notation for dielectric functions is used.

$$\epsilon_i = \begin{cases} \epsilon_i(\omega) & \text{for active medium} \\ \epsilon_i & \text{for inactive medium} \end{cases} \tag{1}$$

where $i = 1, 2, 3$ and for metals, the dielectric function of the form

$$\epsilon_i(\omega) = 1 - \frac{\omega_{pi}^2}{\omega^2} \tag{2}$$

is used, with ω_{pi} representing the plasma frequency.

For the SCSIM system, it is convenient to use the bispherical coordinate system (η, α, ψ) which is related to the rectangular coordinate system (x, y, z) by (see, for

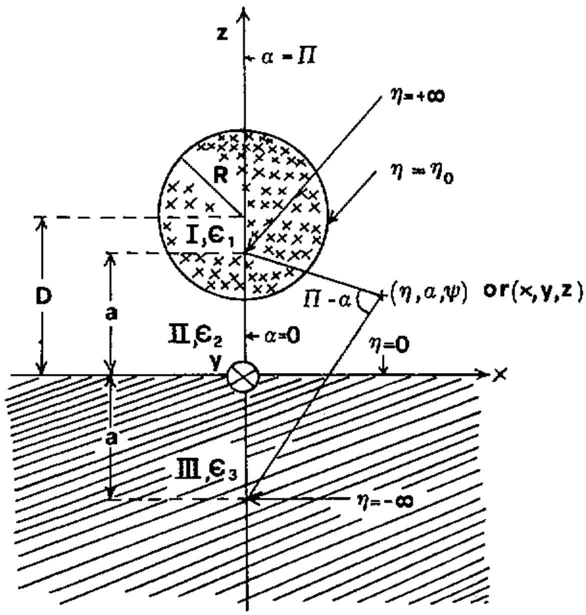

Figure 1. The geometry of a sphere coupled to a semi-infinite medium showing regions I, II and III with dielectric functions ϵ_1, ϵ_2 and ϵ_3. Bispherical coordinates (η, α, ψ) are used to study the system, and $\psi = \tan^{-1}(y/x)$ where the y-axis is into the page plane. All other symbols are defined in the text.

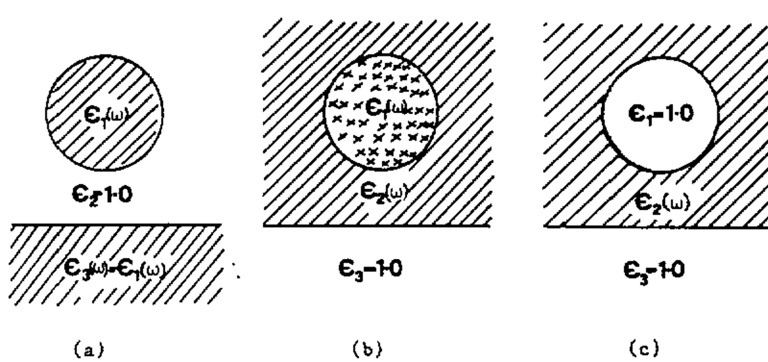

Figure 2. (*a*) A metallic sphere in vacuum coupled to a semi-infinite metal of the same material. (*b*) A metallic sphere embedded into a semi-infinite metal bounded by vacuum. (*c*) A spherical cavity inside a semi-infinite metal bounded by vacuum.

example, Moon and Spencer (1988))

$$x = \frac{a \sin\alpha \cos\psi}{\cosh\eta - \cos\alpha} \tag{3}$$

$$y = \frac{a \sin\alpha \sin\psi}{\cosh\eta - \cos\alpha} \tag{4}$$

$$z = \frac{a \sin h\eta}{\cos h\eta - \cos\alpha} \tag{5}$$

where

$$a = (D^2 - R^2)^{1/2} \tag{6}$$

$$D = a \coth \eta_0. \tag{7}$$

The surface modes we are considering satisfy Laplace's equation.

$$\nabla^2 \phi_i = 0 \tag{8}$$

where $i = 1, 2, 3$ for the solutions in the three regions I, II and III. Equation (8) is valid for the surface modes considered in this paper, and is solved in the non-retarded limit. The solutions are

$$\phi_1 = (\cos h\eta - \cos\alpha)^{1/2} \sum_{n=0}^{\infty} C_n^o \mathrm{e}^{-(n+\frac{1}{2})\eta} P_n(\cos\alpha) \tag{9}$$

$$\phi_2 = (\cosh\eta - \cos\alpha)^{1/2} \sum_{n=0}^{\infty} \{A_n^o \mathrm{e}^{-(n+\frac{1}{2})(\eta-\eta_0)} + B_n^o \mathrm{e}^{(n+\frac{1}{2})(\eta-\eta_0)}\} P_n(\cos\alpha) \tag{10}$$

$$\phi_3 = (\cos h\eta - \cos\alpha)^{1/2} \sum_{n=0}^{\infty} D_n^o \mathrm{e}^{(n+\frac{1}{2})\eta} P_n(\cos\alpha) \tag{11}$$

where $P_n(\cos\alpha)$ are Legendre polynomials. Applying boundary conditions in bispherical coordinates at $\eta = \eta_0$ and $\eta = 0$, we have

$$\phi_1(\eta_0) = \phi_2(\eta_0) \tag{12}$$

$$\epsilon_1 \left(\frac{\partial\phi_1}{\partial\eta}\right)_{\eta_0} = \epsilon_2 \left(\frac{\partial\phi_2}{\partial\eta}\right)_{\eta_0} \tag{13}$$

$$\phi_2(\eta = 0) = \phi_3(\eta = 0) \tag{14}$$

$$\epsilon_2 \left(\frac{\partial\phi_2}{\partial\eta}\right)_{\eta=0} = \epsilon_3 \left(\frac{\partial\phi_3}{\partial\eta}\right)_{\eta=0}. \tag{15}$$

Using equations (12) to (15) and equating coefficients of the Legendre polynomials of order n, and after some algebra, a relation giving the frequency dependence on distance D is obtained

$$[\epsilon_2 - \epsilon_3][\epsilon_2 - \epsilon_1]\mathrm{e}^{-(2n+1)\eta_0} + [\epsilon_2 + \epsilon_3][\epsilon_2 f(n, \eta_0) - \epsilon_1] = 0 \tag{16}$$

where

$$f(n, \eta_0) = \frac{1 + (2n+1)\coth\eta_0}{1 - (2n+1)\coth\eta_0}. \tag{17}$$

Equation (16) is the main result of this paper, and it describes the relation between frequency of surface modes of a SCSIM system and the distance D between the sphere of radius R and the interface of the semi-infinite medium, noting that the parameter η_0 is given by

$$\eta_0 = \coth^{-1}\left(\frac{1}{1-1/s^2}\right)^{1/2} \tag{18}$$

and

$$s = D/R. \tag{19}$$

It is of interest to discuss the following *three* limiting cases of our main result given in equation (16). First, let us consider the limit when the distance between the sphere and the semi-infinite medium gets very large. It can be noted that as $D/R \to \infty$,

$$\coth\eta_0 \to 1 \qquad \eta_0 \to \infty \tag{20}$$

and hence the first term in equation (16) becomes negligible, and the second term implies, either

$$\epsilon_3 = -\epsilon_2 \tag{21}$$

or

$$\epsilon_1/\epsilon_2 = -\left(\frac{n+1}{n}\right) \tag{22}$$

where we have used

$$\lim_{\eta_0\to\infty} f(n,\eta_0) = -\left(\frac{n+1}{n}\right). \tag{23}$$

Equation (21) can be recognized as the condition for the existence of surface modes along the semi-infinite medium and region II interface (see, for example, Cottam and Tilley (1989)), while equation (22) can be recognized as the condition for the existence of surface modes for an isolated sphere (see, for example, Ruppin and Englman (1970)). Thus the expression that has been obtained in equation (16) correctly reproduces the expected results in the limit of large D/R.

Second, our result in equation (16) also explains the behaviour in the low separation limit as $D/R \to 1$, that is the small D limit. This limit is of practical interest as in, for example, the SNOM experiments discussed by Fischer and Pohl (1989), where small protrusions over a gold film were illuminated by a HeNe laser and the scattered intensity was measured. These authors observed that there were narrow resonances which were dependent on the distance between the sphere and the gold film. These resonances could correspond to the surface modes predicted by our equation (16).

Third, consider the limit when $\epsilon_1 \to \infty$ and $\epsilon_2 = 1$. In this limit equation (16) reduces to

$$[1-\epsilon_3]e^{-(2n+1)\eta_0} + [1+\epsilon_3] = 0 \tag{24}$$

which corresponds to the case of a semi-infinite medium bounded by vacuum and a small sphere of an infinite dielectric constant.

3. Numerical results and discussion

In this section we present the numerical results by applying the theory developed in section 2 to three cases of practical interest.

3.1. Case (a): $\epsilon_1(\omega) = \epsilon_3(\omega)$ and $\epsilon_2 = 1.0$

Consider the case illustrated in figure 2(a) in which regions I and III are occupied by an active medium with the *same* dielectric function, and region II is occupied by vacuum. Typical values for the plasma frequency of the metals used are $\omega_{p1} = \omega_{p3} = 10$ eV. Equation (16) is solved numerically and the ratio of the dielectric functions, $\epsilon_1(\omega)/\epsilon_2$, is plotted against D/R in figure 3. The results for the SCSIM system show that there are two surface modes, with the lower mode having values $\epsilon_1(\omega)/\epsilon_2$ of $-2.75, -1.70$ and -1.39 for $n = 1, 2, 3$ respectively when $D/R = 3.0$. The values for an isolated sphere using equation (22) give $\epsilon_1(\omega)/\epsilon_2$ values of $-2, -\frac{3}{2}$ and $-\frac{4}{3}$ for $n = 1, 2, 3$ respectively. These results show that even at $D/R = 3.0$, the lower mode already shows an isolated sphere behaviour. The effects of coupling between the sphere and the semi-infinite medium are strong as $D/R \to 1$, where frequency changes drastically. The upper mode shows that at $D/R = 3.0$ the ratio $\epsilon_1(\omega)/\epsilon_2 = -0.74, -0.87$ and -0.95 for $n = 1, 2, 3$ respectively, while the uncoupled semi-infinite plane has surface modes at $\epsilon_1(\omega)/\epsilon_2 = -1$.

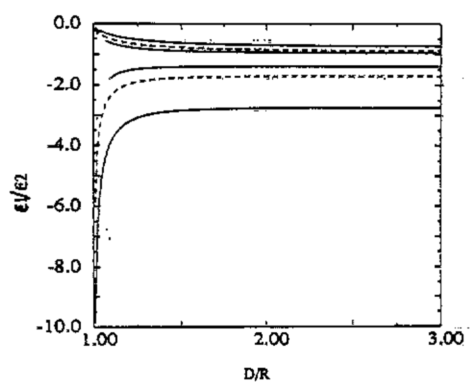

Figure 3. The ratio of dielectric functions $\epsilon_1(\omega)/\epsilon_2$ against reduced distance D/R. Full curve, broken curve and points correspond to $n = 1, 2, 3$, respectively.

In figure 4, the reduced frequency ω/ω_p is plotted against D/R. Two surface modes are found for each order n, with the lower branch increasing with increasing D/R and having values of ω/ω_p as 0.52, 0.61 and 0.65 for $n = 1, 2, 3$ respectively when $D/R = 3.0$ and corresponding values for the upper mode are 0.76, 0.73 and 0.72. These values can be explained by noting that at large distances, the sphere and the semi-infinite medium become uncoupled and isolated sphere frequencies are $\sqrt{1/3}, \sqrt{2/5}$ and $\sqrt{3/7}$ for $n = 1, 2, 3$ respectively using the following equation, which is obtained by using (2) and (22).

$$\frac{\omega_n}{\omega_{p3}} = \sqrt{\frac{n}{n(1+\epsilon_2)+1}}. \tag{25}$$

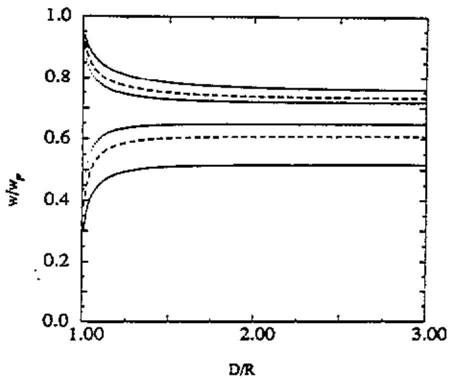

Figure 4. Reduced frequency ω/ω_p is plotted against D/R for a metallic sphere in vacuum coupled to a semi-infinite metal of the same material. Full curve, broken curve and points correspond to $n = 1, 2, 3$, respectively.

The upper mode decreases with increasing D/R, to a limiting value of $\omega/\omega_p = 1/\sqrt{2}$. This can be explained by noting that from (2) and (21), the surface modes along the uncoupled semi-infinite medium satisfy

$$\frac{\omega}{\omega_{p3}} = \frac{1}{\sqrt{1+\epsilon_2}}. \tag{26}$$

3.2. Case (b): $\epsilon_1(\omega) \neq \epsilon_2(\omega)$ and $\epsilon_3 = 1.0$

In this case, as illustrated in figure 2(*b*), a sphere in region I is embedded in region II and these two regions are of active medium with *different* dielectric functions and region III is occupied by vacuum. The results are illustrated by taking plasma frequencies as $\omega_{p1} = 5$ eV and $\omega_{p2} = 10$ eV. In figure 5, a plot of ω/ω_p against D/R shows that there are two branches of surface modes for each order n, with the lower branch increasing with increasing D/R and having values of ω/ω_p as 0.67, 0.70 and 0.70 for $n = 1, 2, 3$ respectively when $D/R = 3.0$ while the upper mode has the values 0.89, 0.84 and 0.83 at the same distance. The interpretation of these values now corresponds to the following: the lower mode approaches the vacuum–plane interface frequencies while the upper mode approaches the isolated sphere frequencies obtained by using equations (2) and (22) to obtain

$$\frac{\omega_n}{\omega_{p2}} = \sqrt{1+\left(\frac{n}{n+1}\right)\frac{\omega_{p1}^2}{\omega_{p2}^2}\Big/\left[1+\left(\frac{n}{n+1}\right)\right]} \tag{27}$$

which predicts values of ω_n/ω_p of 0.87, 0.84 and 0.82 for $n = 1, 2, 3$ respectively, which agrees well with the numerical prediction of equation (16) at $D/R = 3.0$. One observation that has been made for case (c) is that the mode associated with the isolated sphere is the upper mode, and that with the uncoupled plane interface is the lower mode, and this behaviour is different from that of case (a) as discussed in section 3.1.

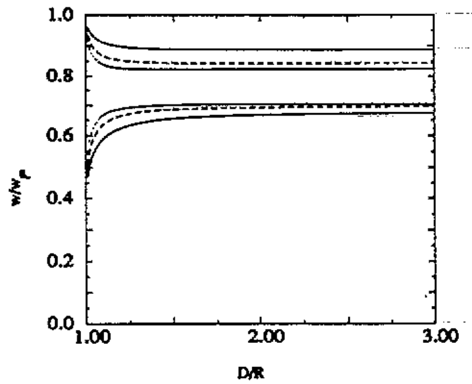

Figure 5. Reduced frequency ω/ω_p is plotted against D/R for a metallic sphere embedded into a semi-infinite metal bounded by vacuum. Full curve, broken curve and point curve correspond to $n = 1, 2, 3$, respectively.

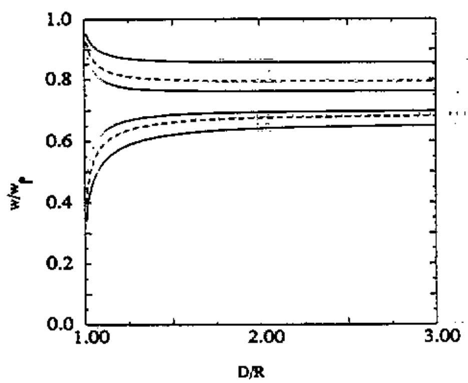

Figure 6. Reduced frequency ω/ω_p is plotted against D/R for a spherical cavity inside a semi-infinite metal bounded by vacuum. Full curve, broken curve and points correspond to $n = 1, 2, 3$, respectively.

3.3. Case (c): $\epsilon_1 = \epsilon_3 = 1.0$ and $\epsilon_2(\omega)$ for region II

Consider the case illustrated in figure 2(*c*), where a spherical inactive region consisting of a void of dielectric constant ϵ_1 in region I which is embedded in region II which is active with a dielectric function $\epsilon_2(\omega)$. On the other side of the interface in region III is vacuum. In figure 6, a graph of ω/ω_p against D/R shows that there are two branches of surface modes, with the lower branch increasing with increasing D/R and having values of ω/ω_p as 0.65, 0.68 and 0.70 for $n = 1, 2, 3$ respectively when $D/R = 3.0$, while the upper mode has reduced frequencies of 0.86, 0.79 and 0.76 at the same distance and the respective values of n are 1, 2 and 3. The upper mode frequencies can be compared with those of an isolated void or bubble with frequencies given by (22) and hence

$$\frac{\omega_n}{\omega_{p2}} = \sqrt{\frac{(n+1)}{n(1+\epsilon_1)+1}} \tag{28}$$

which gives values of the reduced frequencies of $\sqrt{2/3}$, $\sqrt{3/5}$ and $\sqrt{4/7}$ for $n = 1, 2, 3$ respectively. This gives a good prediction of equation (16) at large D/R.

4. Conclusions

The main result of this paper is equation (16), which describes the frequency variation with distance for surface modes of a sphere coupled to a semi-infinite medium. It has been shown that there are two surface modes for every order n, and these orders are the source of a large range of frequencies that would not have been present if the semi-infinite plane was alone, and observations of this effect have been made in surface enhanced Raman scattering (Fleischmann *et al* (1974), Udagawa *et al* (1981), Aravind *et al* (1983), Otto (1984), Moskovits (1985), Takamori *et al* (1987)) and SNOM experiments (Fischer and Pohl (1989)). Three limiting cases of practical interest have been discussed at the end of section 2. First, when the distance between the sphere and the semi-infinite medium becomes very large, equation (16) reduces to the limit of uncoupled modes along the semi-infinite medium and region II interface (see, for example, Cottam and Tilley (1989)), and surface modes for an isolated sphere (see, for example, Ruppin and Englman (1970)). Second, in the limit of small D/R, strong effects of coupling between the sphere and the semi-infinite medium have been illustrated in figures 3 to 6. Third, the case of a sphere with an infinite dielectric constant bounded by vacuum over a semi-infinite medium has been considered in section 2. The model has also been applied to three cases of practical interest in section 3: first, a metallic sphere in vacuum coupled to a semi-infinite metal of the same material; second, a metallic sphere embedded into a semi-infinite metal bounded by vacuum; third, a spherical cavity inside a semi-infinite metal bounded by vacuum. The numerical results that have been presented in this paper show the intrinsic properties of surface modes in the SCSIM system. Suitable experimental techniques for observing these surface modes include Raman scattering, absorption measurements, STM and SNOM as mentioned earlier.

Acknowledgments

The author would like to thank Professor Abdus Salam, the International Atomic Energy Agency, and Unesco for hospitality at the ICTP (International Centre for Theoretical Physics) Trieste, Italy, and Sarec for the associateship scheme at ICTP. Thanks are also due to TWAS for support at the University of Botswana, where some of this work was done.

References

Agranovich V M and Loudon R 1984 *Surface Excitations* (Amsterdam: North-Holland)
Agranovich V M and Mills D L 1982 *Surface Polaritons* (Amsterdam: North-Holland)
Aravind P K and Metiu H 1983 *Surf. Sci* **124** 506–28
Binnig G and Rohrer H 1984 *Physica* B **127** 37–45
Cohen R W, Cody G D, Coutts M D and Abeles B 1973 *Phys. Rev.* B **8** 3689–701
Cottam M G and Tilley D R 1989 *Introduction to Surface and Superlattice Excitations* (Cambridge: Cambridge University Press)
Fischer U C and Pohl D W 1989 *Phys. Rev. Lett.* **62** 458–61
Fleischmann M, Hendra P J and McQuillan A J 1974 *Chem. Phys. Lett.* **26** 163–6
Johnson P B and Christy R W 1974 *Phys. Rev.* **9** 5056–70
Moon P and Spencer D E 1988 *Field Theory Handbook* (Berlin: Springer)
Moskovits M 1985 *Rev. Mod. Phys.* **57** 783–826

Otto A 1984 *Light Scattering in Solids vol IV (Topics in Applied Physics 54)* ed M Cardona and G Guntherodt (Berlin: Springer)
Rendell R N, Scalapino D J and Muhlschlegel B 1978 *Phys. Rev. Lett.* **41** 1746–50
Ruppin R 1983 *Surf. Sci.* **127** 108–18
Ruppin R and Englman R 1970 *Rep. Prog. Phys.* **33** 149–96
Takamori T, Masahiro I and Ohtaka K 1987 *J. Phys. Soc. Japan* **56** 1587–602
Udagawa M, Ching-Cong C, Hemminger J C and Ushioda S 1981 *Phys. Rev.* B **23** 6843–46